Comparing the qualitative performances of handheld NIR and Raman spectrophotometers for the detection of falsified pharmaceutical products

P.H. Ciza[a,b,1], P.-Y. Sacre[a,1]*, C. Waffo[a,c], L. Coïc[a], H. Avohou[a], J.K. Mbinze[b], R. Ngono[c], R.D. Marini[a], Ph. Hubert[a], E. Ziemons[a]

[a] University of Liege (ULiege), CIRM, VibraSante Hub, Department of Pharmacy, Laboratory of Pharmaceutical Analytical Chemistry, Liege, Belgium.

[b] University of Kinshasa, Faculty of Pharmaceutical Sciences, LACOMEDA, Lemba, 212 Kinshasa XI, Democratic Republic of Congo

[c] University of Yaoundé I, Faculty of Medicine and Biomedical Sciences and National Drug Control and Valuation (LANACOME), Cameroon

Abstract:

Over the last decade, the growth of the global pharmaceutical market has led to an overall increase of substandard and falsified drugs especially on the African market (or emerging countries). Recently, several methods using handheld/portable vibrational spectroscopy have been developed for rapid and on-field drug analysis. The objective of this work was evaluate the performances of various NIR and Raman handheld spectrophotometers in specific brand identification of medicines through their primary packaging. Three groups of drug samples (artemether-lumefantrine, paracetamol, and ibuprofen) were used in tablet or capsule forms. In order to perform a critical comparison, the analytical performances of the two analytical systems was compared statistically using three methods: hierarchical clustering algorithm (HCA), data-driven soft independent modeling of class analogy (DD-SIMCA) and hit quality index (HQI). The overall results show good detection abilities for NIR systems compared to Raman systems based on Matthews's correlation coefficients, generally close to one. Raman systems are less sensitive to the physical state of the samples than the NIR systems, it also suffers of the auto-fluorescence phenomenon and the signal of highly dosed active pharmaceutical ingredient (e.g. paracetamol or lumefantrine) may mask the signal of low-dosed and weaker Raman active compounds (e.g. artemether). Hence, Raman systems are less effective for specific product identification purposes but are interesting in the context of

falsification because they allow a visual interpretation of the spectral signature (presence or absence of API).

Keywords: Falsification, Handheld, Near infrared spectroscopy, Raman spectroscopy, DD-SIMCA.

[1]These authors have equally contributed to this article.

*Corresponding Author. Tel.: +32 4 366 4324; Fax: +32 4 366 4317

E-mail address: pysacre@uliege.be

Address: Laboratory of Analytical Pharmaceutical Chemistry, CIRM, VibraSante Hub, Department of Pharmacy, University of Liege, Avenue Hippocrate 15, B-4000 Liege, Belgium

1. Introduction

The significant growth of the pharmaceutical market in emerging countries has led to the emergence of numerous falsifications [1]. Quality promoting programs and research activities has followed this growth but not proportionally [2–4]. Over the past two decades, the United States Agency for International Development (USAID) and United States Pharmacopoeia (USP), based on three cooperation programs, contributed significantly to the improvement of the quality control and quality assurance systems in developing countries [5,6]. These programs involved conducting various training sessions on good manufacturing practices (GMP), registration procedures and drug testing methods to ensure the effectiveness, quality and safety of medicines [6]. The World Health Organization (WHO) estimates that at least 10 % of drugs are falsified or substandard medicines (SF) in low and middle income countries (LMIC) [7–9]. Many efforts are needed to tackle this problematic in the economic, politic and scientific fields.

Detection of poor quality drugs is a major scientific challenge linked to SF. Due to the complexity of situations (absence/wrong active ingredient, wrong amount of active ingredient, too high amount of impurities, bad dissolution profiles, etc.) no single device can actually detect all SF medicines. Several analytical field techniques exist to detect SF drugs and each has its own specificities [10].

Among these techniques, near infrared (NIR) spectroscopy and Raman spectroscopy are more and more used because of their fast, simple and non-destructive features [11–16]. Recently, special attention is focusing on handheld NIR and Raman devices. Indeed, in addition to their miniaturization, these devices may embed intelligent decision-making algorithms and on-board spectral libraries. Clearly, they may offer important advantages over conventional analytical chemistry methods in the detection of SF drugs throughout the supply chain because they allow the development and *in-situ* implementation of several analytical methods [17,18]. These advantages, however depend on their analytical performances (sensitivity and specificity), their cost, and their ability to perform real-time field analyses [19]. Currently, there is a wide variety of handheld spectrophotometers based on vibrational spectroscopy. Nonetheless, their analytical performances in medicine verification issues, compared to benchtop spectrophotometers, remain to be proven. These performances depend not only on the technical features and configurations of the instruments, but also on the accuracy of the spectral data analysis techniques used, among others.

NIR and Raman spectra of pharmaceuticals contain information on both the physical and chemical properties of the sample, which is convolved with extraneous information such as instrument noise, measurement errors, and other interfering signals such as sample auto-fluorescence or scattering [20,21]. Because of these, spectral data require specific preprocessing and decision-making methods to extract the meaningful pieces of information and to take decisions.

In the context of drug product verification three families of chemometric methods are commonly used: spectral correlation methods (e.g. hit quality index referred to as HQI), class modelling methods (e.g. the soft-independent modelling of class analogy referred to as SIMCA) and classification methods (e.g. Partial Least Squares Discriminant Analysis referred to as PLS-DA).

Spectral correlation algorithms are the simplest identification algorithms and are the most frequently embedded in handheld systems. They compute similarity indexes between the analyzed (unknown) spectrum and a reference library [22]. One of these methods is the so-called “Hit Quality Index” (HQI) which is usually computed as the squared Pearson’s correlation coefficient between two spectra [23].

Class modelling or one-class classification (OCC) techniques involve the statistical characterization of a target drug based on calibration spectra and then testing whether new spectra are compatible with the estimated characteristics or not. Soft independent modeling of class analogy (SIMCA) is one of the most used OCC techniques. SIMCA method performs principal component analysis (PCA) on the spectra of the target drug and computes scores for each spectrum on significant principal components [24].

The partial least squares discriminant analysis (PLS-DA) is the most commonly used discrimination/classification algorithm in specific brand identification problems [25,26]. This method uses the principle of PLS regression for a classification purpose, with output values of the PLS model that are categorical (coded labels of the classes to be modelled). The calibrated PLS model can then be used to predict the membership or authenticity of new samples [27,28]. PLS-DA allows the manipulation of highly collinear and noisy data but also the identification of the most important variables [29]. However, the SIMCA model is more rigorous as a specific brand identification method than PLS-DA. Indeed, PLS-DA requires a “non-target” samples has to be modelled. However, to be efficient with new unknown sample spectra, this “non-target” class should cover as much variability as possible that could be encountered in the

future. This may therefore constitute a limitation for the PLS-DA model construction. For a more detailed comparison of SIMCA and PLS-DA for specific brand identification purposes, the reader is referred to [26].

The present study aims at evaluating the performances of various NIR and Raman handheld spectrophotometers in specific brand identification of medicines through their primary packaging. Two different chemometric methods were envisaged, namely the HQI and the SIMCA. The HQI was chosen because of its simplicity. It is embedded in almost every handheld systems and is widely used. In the framework of product identification, class-modelling techniques (e.g. SIMCA) are generally more relevant because they model only the target class whereas classification algorithms (e.g. PLS-DA) require not only the target class but also at least one non-target class (for a one vs rest strategy) [26,30,31].

Beside identification algorithms, clustering methods are also widely used to group samples without *a priori* knowledge. Hierarchical agglomerative clustering (HCA) methods are specific clustering techniques widely used in chemometrics. Starting with clusters of a single spectrum or point, the algorithm proceeds at each step by merging pairs of clusters using a (dis)similarity metric (distance of observations relative to each other) and a linkage criterion (the distance of clusters relative to each other), until all spectra are clustered. Unlike the k-means algorithm which clusters spectra in way that each spectrum belongs to the cluster with the nearest mean, HCA does not require any prior specification of the number of clusters [32–35]. During this study, HCA was performed to compare the information provided by each spectrophotometric technique.

2. Material and methods

2.1. NIR and Raman Instrumentation

The instruments selected and evaluated in the study included:

i. Two NIR systems: a Fourier transform (FT) benchtop (FT-NIR Multi Purpose Analyzer MPA, Bruker Optics, Germany) and a low-cost handheld dispersive spectrophotometer (NIR-SG-1, Tellspec, Canada);
ii. Two handheld Raman device systems: a FDA 21CFR part 11 qualified (TruScan RM, Thermo Scientific, USA) and a middle-cost device (IDRaman mini, Ocean Optics, USA).

These instruments are representative of what may be found on the market in terms of technology and performances (spectral resolution, laser power and price). In addition, the 785nm laser wavelength is the most used configuration for pharmaceutical analyses purposes. The instrumental characteristics of these systems are summarized in Table 1.

The NIR spectra based on MPA were acquired using a probe for solids with 32 scans and a spectral resolution of 8 cm^{-1}. The internal Te-InGaAs detector was used in the 12500-4000 cm^{-1} spectral range. Acquisition parameters of the handheld devices were set to default. The ID-Raman mini was used in the orbital raster scanning (ORS) mode and no baseline correction was performed. Each device was piloted using its built-in software.

2.2. Drug samples

The drug samples included solid dosage forms (tablets or capsules) of paracetamol, ibuprofen and artemether-lumefantrine as described in Table 2.

These three categories of drugs represent three challenging situations for handheld vibrational spectroscopy:

i. Paracetamol and paracetamol combinations formulations samples (denoted "P") were selected firstly because of the high dosage of paracetamol and its high Raman scattering property, and secondly because of its possible combinations with a large variety of low-dosage APIs. The objective is to evaluate whether handheld systems are able to detect small but major formulation changes such as the presence or absence of other low-dosage APIs in the presence of a potentially masking compound.
ii. Ibuprofen-based formulations samples (denoted "I") were selected because of the wide variety of colors and pharmaceutical forms. These parameters can influence the NIR or Raman spectra (auto-fluorescence of colored coating, soft capsules …).
iii. Artemether-lumefantrine formulations samples (denoted "AL") represent one of the most falsified class of antimalarial drugs in developing countries. It was therefore interesting to test whether the various instruments and chemometric methods can effectively discriminate different brands of this formulation. Indeed, lumefantrine is a high Raman scatterer and can potentially mask the signal from artemether and excipients, making it difficult to differentiate between different brands.

One formulation of each category was selected as "genuine" sample and hence considered as target class to be modelled: Dafalgan Forte 1g (paracetamol, "G-P" in table 2), Ibuprofen EG

400mg (ibuprofen, “G-I” in table 2) and Coartem 20/120 (artemether/luméfantrine, “G-AL” in table 2). Six different batches of each formulation were acquired in local pharmacies. Three batches were used as training set to build the SIMCA models and to build the reference spectrum (for the HQI analyses) and the three remaining batches were used as test set to evaluate the model performances.

The other formulations (both branded and generic drugs) were used to mimic high quality fake medicines. Additionally, five falsified batches of artemether-lumefantrine formulations containing none of the declared API were also analyzed (denoted “F”).

All samples were obtained from local pharmacies in Belgium (paracetamol; paracetamol combinations and ibuprofen samples) and in Democratic Republic of Congo (artemether-lumefantrine samples). Artemether-lumefantrine samples were analyzed by HPLC to confirm that all samples were conform in terms of identity of declared API and their amount.

2.3. Data acquisition and processing algorithms

2.3.1. Data acquisition and preprocessing

Samples of tablets and capsules were directly scanned through their blister. The spectra of twenty tablets were recorded for each “genuine” formulation while the spectra of ten tablets were recorded for each of the other formulations. Overall, 60 spectra were used as training set (20 spectra for each of the three “genuine” batches) and 1770 spectra (composed of the three remaining “genuine” batches and all other analyzed samples) were used as test set.

To improve the signal-to-noise ratio, the measured spectra have been preprocessed. First, Savitzky-Golay (SG) smoothing and differentiation filter (second-degree polynomial and first derivative) was applied to remove noise and baseline signals. Second, either unit-area normalization or Standard Normal Variate (SNV) were applied to the smoothed and differentiated signals [36].

2.3.2. Hierarchical clustering method

As mentioned in Section 1, agglomerative hierarchical clustering starts with single-element clusters. The algorithm then proceeds at each step by merging the two most similar clusters into a new bigger cluster. This procedure is iterated until all spectra are grouped into one single big cluster [37]. In this study, the L_1- norm or Manhattan distance was used to measure the similarity between pairs of spectra while the Ward’s method was used to group the two closest

clusters at each step. The objective function to be minimized is the variance-weighted distance between cluster centers. It has been demonstrated that $L_1 -$ norm (and hence the least absolute error) are more appropriate than the $L_2 -$ norm (and the sum of squared errors) in high dimensional data analysis [38,39]. The advantage of this method is that it takes into account not only the distance between the clusters but also the intra-cluster distance [39]. Hierarchical clustering would allow observing the significant differences between the spectrophotometers by focusing much more on the categorization of the samples according to their physical and chemical properties. This justified the choice of paracetamol formulations as sample sets for this method.

2.3.3. Hit Quality Index (HQI) method

The HQI was used to analyze the spectral correlation between the "genuine" spectra and the other spectra for NIR and Raman data sets respectively. The HQI was calculated with the following formula [22,40]:

$$\mathrm{HQI} = \frac{(Reference \cdot Unknown)^2}{(Reference \cdot Reference)(Unknown \cdot Unknown)} \times 100 \qquad \text{Equation 1}$$

where $Reference$ indicates the reference spectrum (the median of the 60 spectra of the training set for the "genuine" formulation), $Unknown$ indicates an individual spectrum of an alternative product under study, and the dot symbolizes the scalar product of the two spectral vectors. The HQI with a value of 100 indicates that the unknown spectrum is identical to the reference spectrum and a value close to zero indicates the dissimilarity with the reference spectrum.

2.3.4. SIMCA method (DD-SIMCA)

As mentioned in Section 1, class modeling, especially the SIMCA model, is more recommended for the verification of the identity of the products [41]. There are numerous approaches to build a SIMCA model. In this study, the data-driven SIMCA (DD-SIMCA) has been used. Like any SIMCA model, the DD-SIMCA first performs a PCA on the calibration spectra of the target class and computes a score distance (SD) and an orthogonal distance for each spectrum based on significant PC dimensions. These distances are used to determine a critical distance, at a given confidence level used as boundary or acceptance area for identification [20,42,43].

Unlike classical SIMCA models however, each type of distance is modelled using a scaled chi-squared χ^2 distribution (rather than Fisher F or Hotelling T^2) whose degree of freedom are estimated with the data. Then the two scaled chi-squared distributions are used to define an

acceptance area for a given type I error, α, or level of confidence $1-\alpha$. This acceptance area was used for classification of new dataset (test sample). All DD-SIMCA models were auto scaled. The number of PCs mainly influences the quality of the classification and determines the complexity of the model [44]. The model parameters (number of PC's and α) were optimized in a sequential way.

2.4. Evaluation of performances of the HQI and the DD-SIMCA

The HQI and the DD-SIMCA methods were evaluated for their brand identification performances. Several criteria are used to evaluate the performance of binary classifiers, including the sensitivity, the specificity, the accuracy, the $F1$-score and the Matthews correlation coefficient. The Mathews correlation coefficient (MCC) was preferred since it allows a complete evaluation of the effectiveness of a model, taking into account all possible classification outcomes [31]. It is calculated as:

$$MCC = \frac{TP \times TN - FP \times FN}{\sqrt{(TP+FP)(TP+FN)(TN+FP)(TN+FN)}} \qquad \text{Equation 2}$$

where TP is the number of true positive, that is the spectra of the target class that are correctly classified, FN is the number of false negatives, that is the spectra of the target class that are wrongly classified outside the target class; FP is the number of false positives, that is the spectra of non-target classes that are wrongly classified as belonging to the target class; TN is the number of true negative, that is the spectra of the non-target classes that are correctly classified outside the target class. The MCC value can vary between -1 when all spectra are wrongly classified and $+1$, when all spectra are correctly classified. A value of zero indicates a random assignment of spectra. The main advantage of Matthews correlation coefficient over accuracy or $F1$ score is that it takes into account the class balance ratio and is less affected by unbalanced classes [45].

The MCC, TP, TN, FP, FN values were computed taking only into account the test samples related to each "genuine" class of samples (AL, I and P test samples for G-AL, G-I and G-P models respectively). This was done to avoid over-optimistic results due to the inclusion of easily discriminated of formulations with the wrong API.

3. Results and discussion

3.1.Spectral preprocessing

Figure 1 illustrates the pretreated selected spectral range prior to the modelling process. The first derivative was chosen to remove baseline artifacts (e.g. auto-fluorescence of samples) or scattering light and to enhance small spectral features. Normalization was also applied in order to smooth differences in intensity that are less relevant for qualitative purposes.

3.2.Comparison of performance of NIR and Raman systems using HQI.

Before applying HQI analysis, the spectra were preprocessed as mentioned in Table 3. The reference spectrum for each genuine sample is the median spectrum of the 60 spectra of the training set. An HQI threshold value of 95% was used for a similarity acceptance decision in the database. HQI values comprised between 90 and 95% were also highlighted as warning values demonstrating a high spectral similarity. Usually, HQI analysis is not performed on NIR data because of the broad spectral bands potentially leading to confusing results. However, it was decided to apply exactly the same approach on NIR and Raman data for a better comparison. Nevertheless, the HQI results obtained with NIR data were relatively satisfactory compared to Raman results. Indeed, the MCC of NIR devices is always higher compared to the MCC obtained for Raman devices (see table 3).

The calculated HQI values for each spectral dataset are shown in supplementary Table S.1. The values are reported with their standard deviation when applicable. HQI appears to be easy to compute and effective to detect wrong API samples. However, the sensitivity of the method to small spectral changes due to API combinations or changes in the medicine composition (different excipients for the different brands) is not satisfactory. Indeed, the majority of samples of a same category (P or AL) shows a HQI value above 90% except for the ibuprofen sample because of the formulation differences (soft capsules vs tablets, pink vs white coating, …) that are large enough to enable a differentiation. Surprisingly, the HQI approach leads to relatively satisfactory results for the P and I samples with the NIR devices.

These results of the HQI method confirm that this technique should only be used as a pre-screening technique to detect major differences between samples (wrong or absent API). However, it is not suitable to identify samples having similar formulations.

3.3. Comparison of performance of NIR and Raman systems using DD-SIMCA

DD-SIMCA models were built on each preprocessed data as described in Table 4. Figures of merit of the different models are shown in Table 4. The acceptance plots for the G-AL models

are shown in Fig.2 and for the G-I and G-P models are presented in supplementary figures Fig.S.1 and Fig.S.2, respectively.

As one may observe, the DD-SIMCA models applied on NIR data allowed a perfect (or almost perfect for G-P model on NIR-B device) discrimination and specific brand identification in the three cases studied.

Raman-A device has satisfactory results for G-I and G-P models with MCC higher than 0.9 but unsatisfactory results for G-AL (MCC below 0.5). On the other hand, Raman-B device has mitigated to unsatisfactory results for both models. These results may be explained by the better spectral resolution of device Raman-A enabling the detection of smaller differences.

Although SIMCA is recognized as a powerful discriminant method, especially for specific brand identification purposes, Raman systems have a practical difficulty in showing a spectral difference between different product brands, especially when it contains fluorescent compounds or weak Raman scattering compounds. The results of DD-SIMCA appear to be similar to those obtained using hierarchical clustering algorithm and HQI method. All these methods show that Raman spectroscopy are less sensitive to the physical properties of the samples than NIR spectroscopy, but are strongly influenced by all the chemical properties of the samples.

These results demonstrate that for specific product identification purpose, NIR spectroscopy is more appropriate than Raman spectroscopy. Indeed, it is less sensitive to sample color and other irrelevant information while keeping a good balance of light absorption between compounds avoiding masking effects of highly dosed API's (e.g. lumefantrine or paracetamol).

One of the main drawbacks of NIR spectroscopy is the difficulty of interpretation of the data. Indeed, the SIMCA model might reject a sample even if it contains the correct API but its dosage is different or even its moisture content is different from the calibration set. This leads to confuse situations on the field and the inference of the rejection by the model is almost impossible by field inspectors.

Raman spectra are much easier to interpret and interesting information may be directly obtained on the field (e.g. identification of a wrong API, etc.). This information may lead to direct actions and risk evaluation. Furthermore, Raman spectroscopy is less sensitive to moisture, which may be an advantage in tropical areas since NIR spectroscopy may be influenced by ambient humidity [46].

In formulations containing paracetamol the amount of excipients is very low (~10-15% W/W) and the Raman scattering power of paracetamol is very high so excipients are almost invisible to Raman devices. This explains that Raman spectrophotometers have poor brand identification for paracetamol containing samples.

On the other hand, artemether/lumefantrine formulations have about 40-60% W/W of excipients. This should facilitate the discrimination of different brands based on their Raman spectra. However, lumefantrine is a very high Raman scatterer and may mask other compounds such as artemether but also the excipients depending on their nature (e.g. starch is a weaker Raman scatterer than lactose etc.). Therefore, it is interesting to see in figure 2 that several formulations (with possibly very different excipients) are not distinguished by Raman spectroscopy. Unfortunately, it was not possible to obtain the qualitative composition (nature of the excipients) of all the artemether/lumefantrine formulations to discuss this point.

Finally, ibuprofen formulations may contain between 20-60% W/W of excipients. Nevertheless, as ibuprofen is a moderate Raman scatterer and because very different galenics exist (soft capsules, sugar coated tablets, colorful coatings), it is easier to distinguish them using a Raman spectrophotometer. However, it is important to notice that the signal obtained may not always enable the identification of the API (e.g. for sugar coated tablets (I9 to I13), only the signal from the sugar is obtained).

3.4. Comparison of performances of NIR and Raman systems using HCA.

The dendrograms in Figure 3 compare the clustering of the various samples by the various instruments. Each end of the branch represents a spectrum of a class as described in Table 2. One may observe that the dendrograms obtained from the NIR systems are almost similar to each other and much more different to those obtained with Raman systems. On the one hand, the NIR based dendrograms (Fig.3.A and Fig.3.B) seem to be largely influenced by both the physical and the chemical properties of the samples. For example, the upper internal node of the dendrogram obtained with the NIR-A device (Fig.3.A) represents the division of the dataset of paracetamol formulations. The red branch indicates that the outgoing left branch of this node consists of observations related to samples containing only paracetamol and with transparent blisters while the right gray node is composed of the remaining observations (paracetamol combined with other APIs). This gray branch is divided in two parts. This division may be explained by the composition of the blister (opaque or transparent blister). The branch with the transparent blister then splits according to the solid state of the samples (capsules or tablets).

Finally, the last divisions of each principal branch are related to the chemical composition of the samples (paracetamol with others APIs, e.g.: tramadol, aspirin, caffeine, chlorphenamine maleate). On the other hand, analyzing the dendrograms obtained with Raman systems (Figs.3.C and Fig.3.D), it appears that Raman devices are less sensitive to the physical state of the samples than the NIR systems, but strongly influenced by the phenomenon of auto-fluorescence and highly dosed API masking the signal of lower doses of poor Raman scattering compounds. The Raman-B device dendrogram shows an upper class (in green) on the left, characterizing the combined formulation of paracetamol, aspirin and caffeine; and a lower class (in red) on the right characterized by the different formulations of paracetamol. In addition, branch tips of different classes representing paracetamol only formulations are condensed forming compact blocks suggesting homogeneous observations. Other samples such as the P9 or some batches of P8 show high auto-fluorescence levels due to yellow blister (for P9) and cellulose derivatives (for P8).

Conclusion

In the framework of falsification and based on this study, it is obvious that there is no ideal vibrational spectrophotometer. The choice of a system would depend much more on the final objectives of the analysis. Despite some important limitations (limited number of falsified medicines, use of different brands of genuine medicines to mimic high quality falsified medicines, no evaluation of substandard drugs, absence of verification of the medicines purchased in Belgian pharmacies), some general lessons may be drawn to help the analyst choosing the right technology for the right application.

For specific product identification purpose, NIR devices are preferable. Their performances are much more reliable than Raman counterparts are. Furthermore, the low-cost devices offer promising performance almost comparable to benchtop systems [47]. The main drawback at this time is the need for a complementary system (smartphone, tablet or computer) to pilot and collect the data. The mobile applications are available on most platforms but not suited for pharmaceutical products identification at this time.

Raman devices are less effective in terms of brand identification and discrimination but more interesting in the chemical interpretation of the presence or absence of active pharmaceutical ingredient. This lack of sensitivity to detect differences in formulation may be an advantage in

the framework of substandard drugs. Indeed, it should be possible to build a quantitative model for several formulations and detect out of specification API dosage. Unfortunately, actual default configuration of devices does not allow the user to set acquisition parameters.

As a conclusion, handheld vibrational spectroscopy devices are promising tools in the frame of substandard and falsified drugs identification. However, further work is needed to enable and

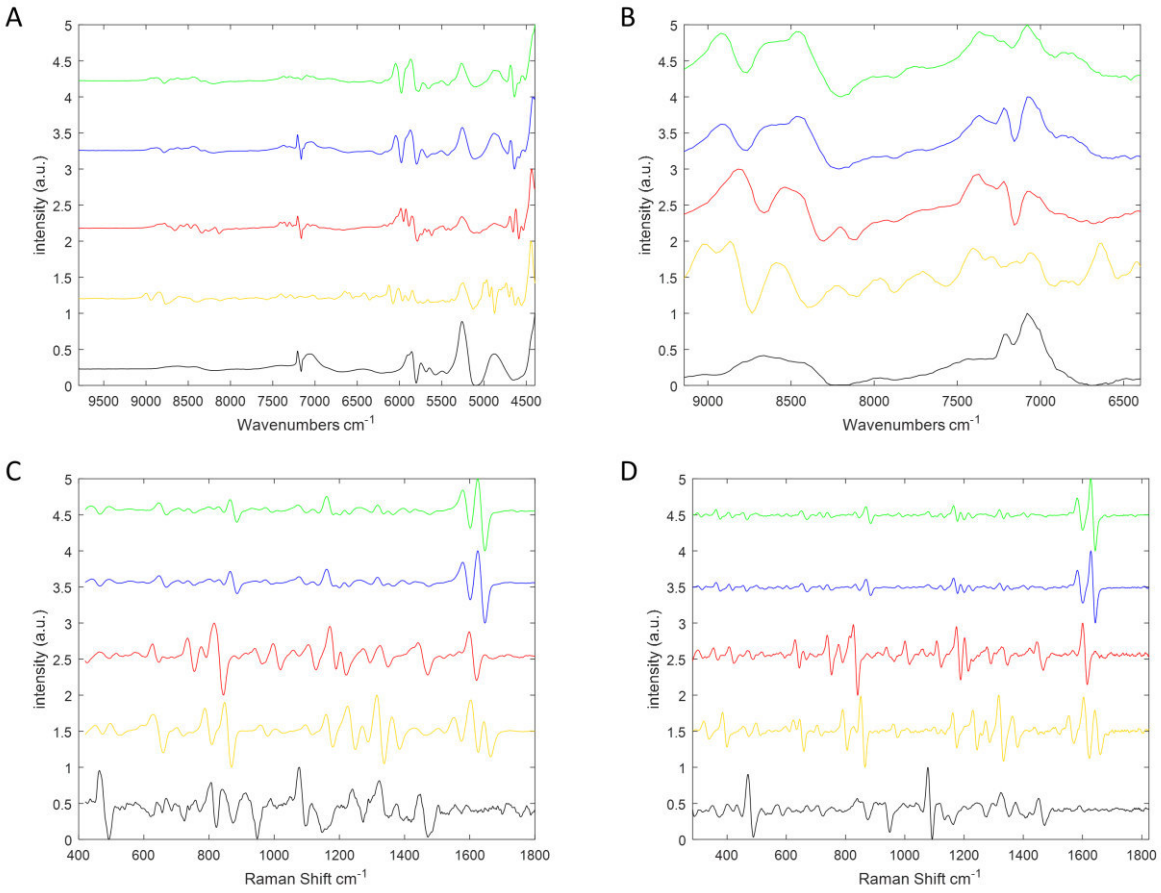

Acknowledgments

This work was done with the financial support of the Academy of Research and Higher Education is the federation of French-speaking higher education institutions in Belgium (ARES). We thank the coordination team of PFS-2016 project.

The authors would also like to thank Dr. Trésor Kimbeni Malongo from the LACOMEDA for providing samples used in this study.

The financial support of this research by the Walloon Region of Belgium in the framework of the Vibra4Fake project (convention n°:7517) is gratefully acknowledged.

The reviewers are acknowledged for the valuable comments that improved the manuscript.

References

[1] M. Tannoury, Z. Attieh, The Influence of Emerging Markets on the Pharmaceutical Industry, (2017). doi:10.1016/j.curtheres.2017.04.005.

[2] E.F.M. ‘t Hoen, H. V Hogerzeil, J.D. Quick, H.B. Sillo, A quiet revolution in global public health: The World Health Organization’s Prequalification of Medicines Programme, J. Public Health Policy. 35 (2014) 137–161. doi:10.1057/jphp.2013.53.

[3] K. Yao, B. McKinney, A. Murphy, P. Rotz, W. Wafula, H. Sendagire, S. Okui, J.N. Nkengasong, Improving Quality Management Systems of Laboratories in Developing Countries, Am. J. Clin. Pathol. 134 (2010) 401–409. doi:10.1309/AJCPNBBL53FWUIQJ.

[4] J.M. Caudron, N. Ford, M. Henkens, C. Mace, R. Kiddle-Monroe, J. Pinel, Substandard medicines in resource-poor settings: a problem that can no longer be ignored, Trop Med Int Heal. 13 (2008) 1062–1072. doi:10.1111/j.1365-3156.2008.02106.x.

[5] Strengthening Manufacturing Capacity to Improve Access to Quality-Assured Essential Medicines About PQM, 2017. http://www.usp-pqm.org/sites/default/files/pqms/article/manufacturing-final-dec2017.pdf.

[6] Ensuring the Quality of Medicines in Resource-Limited Countries World Health Organization National Drug Authority of Uganda · Program for Appropriate Technology in Health National Pharmaceutical Control Bureau of Malaysia · National Institute for Drug Qua, (2007).

[7] T. Kelesidis, I. Kelesidis, P.I. Rafailidis, M.E. Falagas, Counterfeit or substandard antimicrobial drugs: a review of the scientific evidence, J Antimicrob Chemother. 60 (2007) 214–236. doi:10.1093/jac/dkm109.

[8] H. Rebiere, P. Guinot, D. Chauvey, C. Brenier, Fighting falsified medicines: The analytical approach, J. Pharm. Biomed. Anal. 142 (2017) 286–306. doi:10.1016/j.jpba.2017.05.010.

[9] K. Ludasi, T. Sovány, O. Laczkovich, B. Hopp, T. Smausz, G. Regdon, Unique laser coding technology to fight falsified medicines, Eur. J. Pharm. Sci. 123 (2018) 1–9. doi:10.1016/j.ejps.2018.07.023.

[10] S. Vickers, M. Bernier, S. Zambrzycki, F.M. Fernandez, P.N. Newton, C. Caillet, Field detection devices for screening the quality of medicines: a systematic review, BMJ Glob. Heal. 3 (2018) e000725. doi:10.1136/bmjgh-2018-000725.

[11] G.M.L. Nayyar, J.G. Breman, J.E. Herrington, The Global Pandemic of Falsified Medicines: Laboratory and Field Innovations and Policy Perspectives, Am. J. Trop. Med. Hyg. 92 (2015) 2–7. doi:10.4269/ajtmh.15-0221.

[12] S. Kovacs, S.E. Hawes, S.N. Maley, E. Mosites, L. Wong, A. Stergachis, Technologies for detecting falsified and substandard drugs in low and middle-income countries, PLoS One. 9 (2014). doi:10.1371/journal.pone.0090601.

[13] G. Reich, Near-infrared spectroscopy and imaging: Basic principles and

pharmaceutical applications, Adv. Drug Deliv. Rev. 57 (2005) 1109–1143. doi:10.1016/j.addr.2005.01.020.

[14] K. Dégardin, A. Guillemain, N.V. Guerreiro, Y. Roggo, Near infrared spectroscopy for counterfeit detection using a large database of pharmaceutical tablets, J. Pharm. Biomed. Anal. 128 (2016) 89–97. doi:10.1016/j.jpba.2016.05.004.

[15] J.K. Mbinze, P.-Y. Sacré, A. Yemoa, J. Mavar Tayey Mbay, V. Habyalimana, N. Kalenda, P. Hubert, R.D. Marini, E. Ziemons, Development, validation and comparison of NIR and Raman methods for the identification and assay of poor-quality oral quinine drops, J. Pharm. Biomed. Anal. 111 (2015) 21–27. doi:10.1016/j.jpba.2015.02.049.

[16] T. Casian, A. Reznek, A. Loredana Vonica-Gligor, J. Van Renterghem, T. De Beer, I. Tomuță, Development, validation and comparison of near infrared and Raman spectroscopic methods for fast characterization of tablets with amlodipine and valsartan, (2017). doi:10.1016/j.talanta.2017.01.092.

[17] S. Modroño, A. Soldado, A. Martínez-Fernández, B. de la Roza-Delgado, Handheld NIRS sensors for routine compound feed quality control: Real time analysis and field monitoring, Talanta. 162 (2017) 597–603. doi:10.1016/J.TALANTA.2016.10.075.

[18] Handheld Analyzers for the Screening of Pharmaceutical Counterfeits, n.d.

[19] K. Dégardin, A. Guillemain, Y. Roggo, Comprehensive Study of a Handheld Raman Spectrometer for the Analysis of Counterfeits of Solid-Dosage Form Medicines, J. Spectrosc. 2017 (2017). doi:10.1155/2017/3154035.

[20] O.Y. Rodionova, K.S. Balyklova, A.V. Titova, A.L. Pomerantsev, Application of NIR spectroscopy and chemometrics for revealing of the 'high quality fakes' among the medicines, Forensic Chem. 8 (2018) 82–89. doi:10.1016/j.forc.2018.02.004.

[21] S. Neuberger, C. Neusüß, Determination of counterfeit medicines by Raman spectroscopy: Systematic study based on a large set of model tablets., J. Pharm. Biomed. Anal. 112 (2015) 70–78. doi:10.1016/j.jpba.2015.04.001.

[22] J.D. Rodriguez, B.J. Westenberger, L.F. Buhse, J.F. Kauffman, Quantitative evaluation of the sensitivity of library-based Raman spectral correlation methods, Anal Chem. 83 (2011) 4061–4067. doi:10.1021/ac200040b.

[23] S. Lee, H. Lee, H. Chung, New discrimination method combining hit quality index based spectral matching and voting, Anal. Chim. Acta. 758 (2013) 58–65. doi:10.1016/j.aca.2012.10.058.

[24] S. Wold, Pattern recognition by means of disjoint principal components models, Pattern Recognit. 8 (1976) 127–139. doi:10.1016/0031-3203(76)90014-5.

[25] A. Telaar, K.H. Liland, D. Repsilber, G. Nürnberg, An Extension of PPLS-DA for Classification and Comparison to Ordinary PLS-DA, PLoS One. 8 (2013) e55267. doi:10.1371/journal.pone.0055267.

[26] A.L. Pomerantsev, O.Y. Rodionova, Multiclass partial least squares discriminant analysis: Taking the right way-A critical tutorial, J. Chemom. (2018) e3030. doi:10.1002/cem.3030.

[27] J.A. Westerhuis, H.C.J. Hoefsloot, S. Smit, D.J. Vis, A.K. Smilde, E.J.J. van Velzen, J.P.M. van Duijnhoven, F.A. van Dorsten, Assessment of PLSDA cross validation, Metabolomics. 4 (2008) 81–89. doi:10.1007/s11306-007-0099-6.

[28] K.H. Liland, U.G. Indahl, Powered partial least squares discriminant analysis, J. Chemom. 23 (2009) 7–18. doi:10.1002/cem.1186.

[29] L.C. Lee, C.-Y. Liong, A.A. Jemain, Partial least squares-discriminant analysis (PLS-DA) for classification of high-dimensional (HD) data: a review of contemporary practice strategies and knowledge gaps, Analyst. (2018). doi:10.1039/C8AN00599K.

[30] O.Y. Rodionova, A. V. Titova, A.L. Pomerantsev, Discriminant analysis is an inappropriate method of authentication, TrAC Trends Anal. Chem. 78 (2016) 17–22. doi:10.1016/j.trac.2016.01.010.

[31] P. Oliveri, G. Downey, Multivariate class modeling for the verification of food-authenticity claims, TrAC - Trends Anal. Chem. 35 (2012) 74–86. doi:10.1016/j.trac.2012.02.005.

[32] A. Singh, K-means with Three different Distance Metrics, 2013.

[33] G. James, D. Witten, T. Hastie, R. Tibshirani, Springer Texts in Statistics An Introduction to Statistical Learning, n.d.

[34] D. Xu, Y. Tian, A Comprehensive Survey of Clustering Algorithms, Ann. Data Sci. 2 (2015) 165–193. doi:10.1007/s40745-015-0040-1.

[35] J.P. Ortega, M. Del Rocío, B. Rojas, M.J. Somodevilla García, Research issues on K-means Algorithm: An Experimental Trial Using Matlab, n.d.

[36] Åsmund Rinnan, F. van den Berg, S.B. Engelsen, Review of the most common pre-processing techniques for near-infrared spectra, TrAC Trends Anal. Chem. 28 (2009) 1201–1222. doi:10.1016/j.trac.2009.07.007.

[37] M. Gagolewski, M. Bartoszuk, A. Cena, Genie: A new, fast, and outlier-resistant hierarchical clustering algorithm, Inf. Sci. (Ny). 363 (2016) 8–23. doi:10.1016/J.INS.2016.05.003.

[38] C.C. Aggarwal, A. Hinneburg, D.A. Keim, On the Surprising Behavior of Distance Metrics in High Dimensional Space, (2001) 420–434. doi:10.1007/3-540-44503-X_27.

[39] T. Strauss, M.J. von Maltitz, Generalising Ward's Method for Use with Manhattan Distances., PLoS One. 12 (2017) e0168288. doi:10.1371/journal.pone.0168288.

[40] Spectral Preprocessing for Raman Library Searching | American Pharmaceutical Review - The Review of American Pharmaceutical Business & Technology, (n.d.).

[41] O.Y. Rodionova, P. Oliveri, A.L. Pomerantsev, Rigorous and compliant approaches to one-class classification, Chemom. Intell. Lab. Syst. 159 (2016) 89–96. doi:10.1016/j.chemolab.2016.10.002.

[42] A.L. Pomerantsev, O.Y. Rodionova, Concept and role of extreme objects in PCA/SIMCA, J. Chemom. 28 (2013) n/a-n/a. doi:10.1002/cem.2506.

[43] A.L. Pomerantsev, O.Y. Rodionova, On the type II error in SIMCA method, J. Chemom. 28 (2014) 518–522. doi:10.1002/cem.2610.

[44] Y. V Zontov, O.Y. Rodionova, S. V Kucheryavskiy, A.L. Pomerantsev, DD-SIMCA — A MATLAB GUI tool for data driven SIMCA approach, Chemom. Intell. Lab. Syst. 167 (2017) 23–28. doi:10.1016/j.chemolab.2017.05.010.

[45] S. Boughorbel, F. Jarray, M. El-Anbari, Optimal classifier for imbalanced data using Matthews Correlation Coefficient metric, PLoS One. 12 (2017) 1–17. doi:10.1371/journal.pone.0177678.

[46] S.H.F. Scafi, C. Pasquini, Identification of counterfeit drugs using near-infrared spectroscopy, Analyst. 126 (2001) 2218–2224. doi:10.1039/b106744n.

[47] R. Deidda, P.-Y. Sacre, M. Clavaud, L. Coïc, H. Avohou, P. Hubert, E. Ziemons, Vibrational spectroscopy in analysis of pharmaceuticals: Critical review of innovative portable and handheld NIR and Raman spectrophotometers, TrAC Trends Anal. Chem. 114 (2019) 251–259. doi:10.1016/j.trac.2019.02.035.

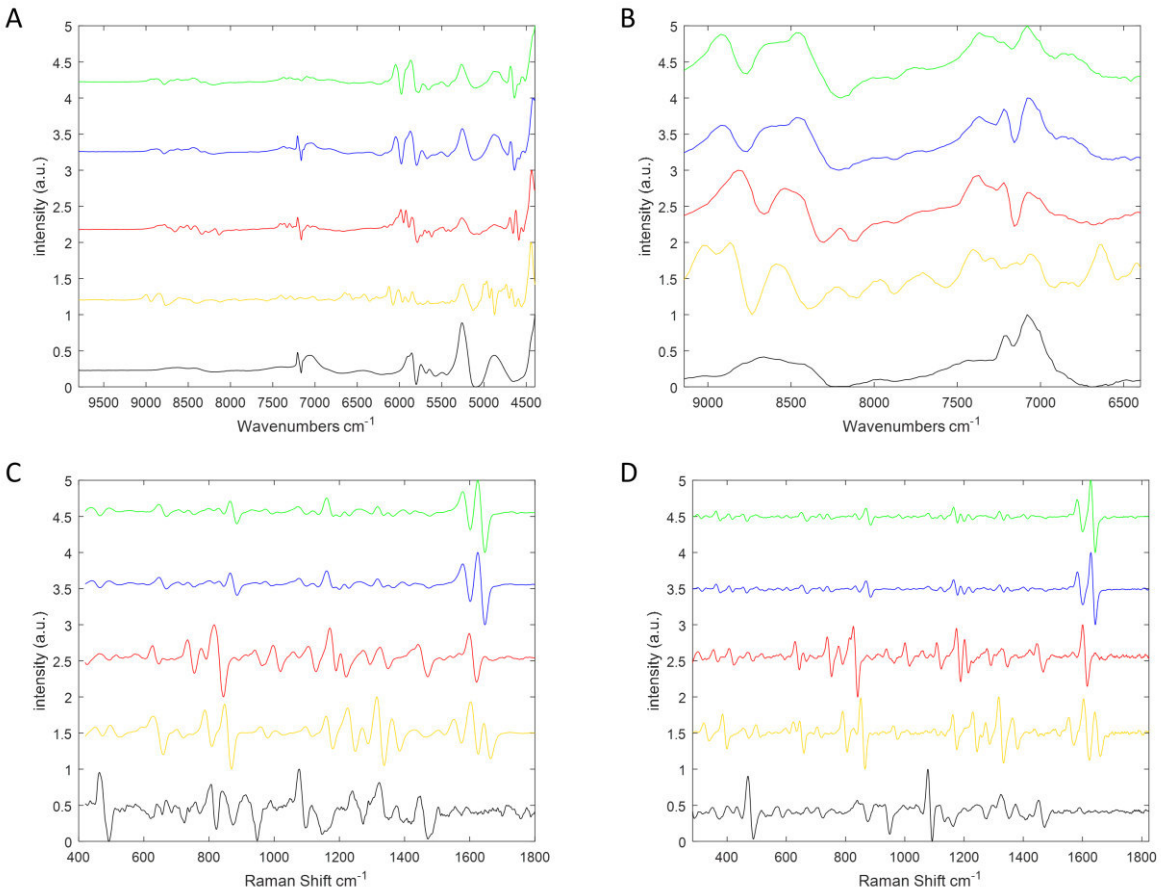

Fig 1. (A) NIR-A pre-processed spectra; (B) NIR-B pre-processed spectra ; (C) Raman-A pre-processed spectra ; (D) Raman-B preprocessed spectra.. The preprocessing of the spectra is the same as presented in Table 3. Green spectra are the median G-AL, blue spectra are the median AL, red spectra are the median I, yellow spectra are the median P and black spectra are the median C.

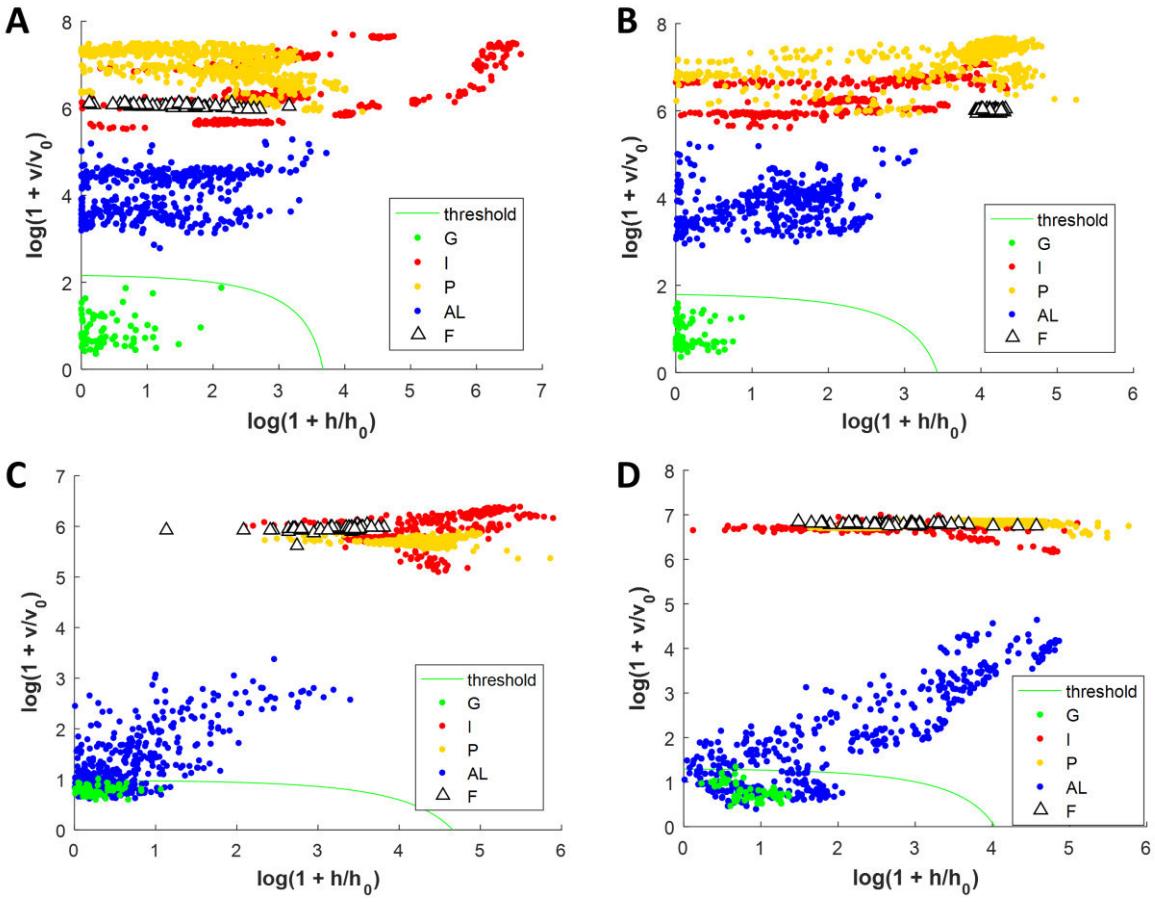

Fig. 2. G-AL DD-SIMCA acceptance plots: (A) NIR-A (B) NIR-B (C) Raman-A (D) Raman-B. “G” samples are the reference artemether-lumefantrine samples; “I” samples are the ibuprofen samples; “P” samples are the paracetamol and paracetamol combination samples; “AL” samples are the artemether-lumefantrine samples and “F” samples are the falsified samples (for more details the reader is referred to Table 2).

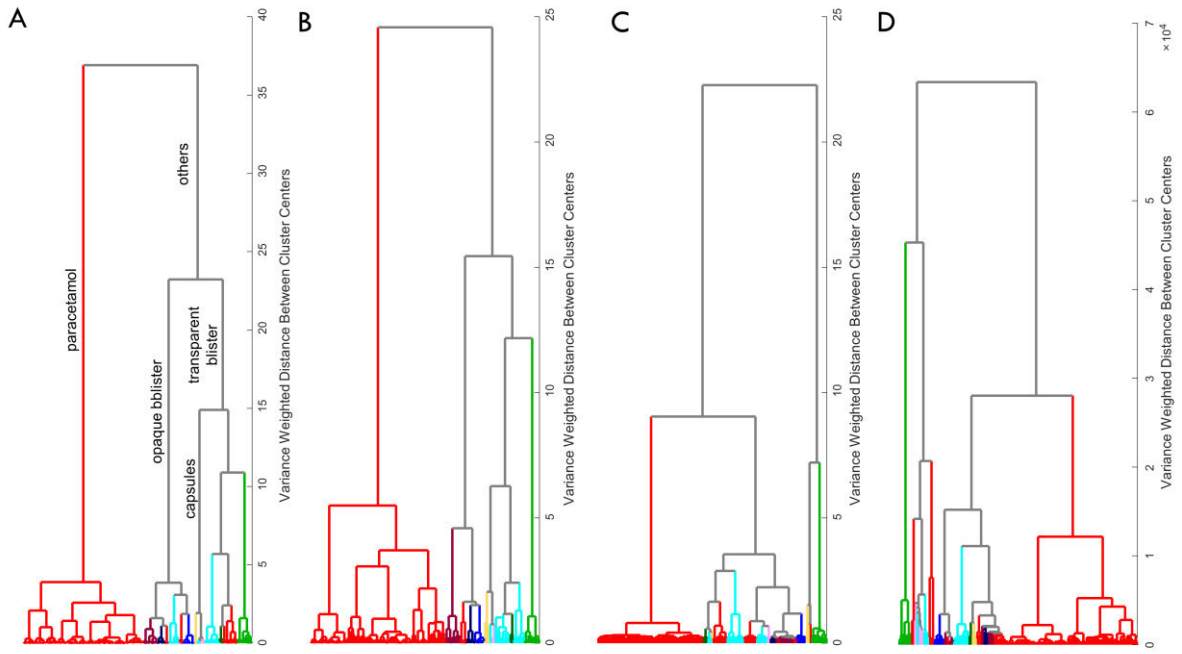

Fig 3. (A) NIR-A dendrogram of data with mean center using Ward method + Manhattan distance; (B) NIR-B dendrogram of data with mean center using Ward method + Manhattan distance; (C) Raman-A dendrogram of data using Ward method + Manhattan distance ; (D) Raman-B dendrogram of data using Ward method + Manhattan distance.

Table 1 : characteristics of NIR and Raman spectrophotometers

Code name	Vibrational spectroscopy	Manufacturer	Model	spectral range analysed (cm^{-1})	data points	pixel resolution (cm^{-1}) [a]	spectral resolution (cm^{-1}) [b]	Weight (kg)	price (k€)
NIR A	FT-NIR	Bruker Optics	MPA (solid probe)	12493 - 400	2203	5.5	N/A	benchtop	~ 100
NIR B	dispersive NIR	Tellspec Inc.	NIR-S-G1	11111 - 5882	256	20.4	N/A	0.14	~ 1,4
Raman A	Raman (785 nm)	Thermo Fisher Inc.	Truscan RM	250 - 2875	2020	1.3	13.3	0.9	~ 60
Raman B	Raman (785 nm)	Ocean Optics Inc.	IDRaman version 1	400 - 2300	1901	1	28.9	0.35	~ 17

[a] computed as the analsed spectral range divided by the number of data points

[b] computed following the ASTM E2529-06 guidance

Table 2 : Description of analyzed samples

Code	Active Pharmaceutical Ingredient	Brand Name	Dosage (mg)	Galenic forms	Test Batches
G-AL	lumefantrine/artemether	Coartem	120/20	Tablets	3
G-P	paracetamol	Dafalgan Forte	1000	Tablets	3
G-I	ibuprofen	Ibuprofen EG	400	Tablets	3
P1	paracetamol	Algostase Mono	1000	tablets	1
P2	paracetamol	Dafalgan	500	tablets	4
P3	paracetamol	Dafalgan Forte	1000	coated tablets	4
P4	paracetamol	Panadol	500	tablets	2
P5	paracetamol	Panadol retard	665	modified release tablets	4
P6	paracetamol	Paracétamol EG	1000	coated tablets	4
P7	paracetamol	Paracétamol EG	500	coated tablets	4
P8	paracetamol	Paracetamol Mylan	500	tablets	1
P9	paracetamol	Paracetamol Tech EMI	500	tablets	1
P10	paracetamol	Paracetamol Teva	500	tablets	3
P11	paracetamol	Paracetamol Teva	1000	tablets	11
P12	paracetamol	Perdolan	500	tablets	4
P13	paracetamol/acetylsalicylic acid/cafeine	Excedryn	250/250/65	coated tablets	4
P14	paracetamol/cafeine	Panadol plus	500/65	coated tablets	3
P15	paracetamol/chlorphenamine maleate	Rhinofebryl	240/3.2	hard capsules	1
P16	paracetamol/codeine	Dafalgan codeine	500/30	coated tablets	1
P17	paracetamol/dextropropoxyphene	Algophene SMB	30/400	hard capsules	1
P18	paracetamol/pseudoephedrine	Sinutab	500/30	tablets	1
P19	paracetamol/pseudoephedrine	Sinutab forte	500/60	tablets	1
P20	paracetamol/tramadol	Algotra	37.5/325	coated tablets	1
P21	paracetamol/tramadol	tramadol/paracetamol EG	37.5/326	coated tablets	2
P22	paracetamol/tramadol	tramadol/paracetamol Teva	37.5/327	tablets	4
P23	paracetamol/tramadol	Zaldiar	37.5/328	tablets	1
I1	ibuprofen	Ibucaps	400	soft capsules	2
I2	ibuprofen	Brufen Forte	600	coated tablets	2
I3	ibuprofen	Brufen Retard	800	modified release tablets	2
I4	ibuprofen	Ibuprofen EG	200	coated tablets	1
I5	ibuprofen	Ibuprofen EG	400	coated tablets	2
I6	ibuprofen	Ibuprofen EG	600	coated tablets	8
I7	ibuprofen	Ibuprofen EG	800	coated tablets	1
I8	ibuprofen	Ibuprofen sandoz	400	coated tablets	1
I9	ibuprofen	Ibuprofen TEVA	200	coated tablets	1
I10	ibuprofen	Ibuprofen TEVA	400	coated tablets	1
I11	ibuprofen	Ibuprofen TEVA	600	coated tablets	1
I12	ibuprofen	Nurofen	200	coated tablets	5
I13	ibuprofen	Nurofen	400	coated tablets	4
I14	ibuprofen	Nurofen Fastcaps	400	soft capsules	5
AL1	lumefantrine/artemether	Artefan	20/120	tablets	7
AL2	lumefantrine/artemether	Cartef DS	480/80	tablets	1
AL3	lumefantrine/artemether	Cether-L	480/80	tablets	1
AL4	lumefantrine/artemether	Coartem	120/20	tablets	1
AL5	lumefantrine/artemether	Coartem D	120/20	dispersible tablets	4
AL6	lumefantrine/artemether	Co-Artluf	120/20	tablets	1
AL7	lumefantrine/artemether	Co-Rimétar	480/80	tablets	2
AL8	lumefantrine/artemether	L-Artem	120/20	tablets	3
AL9	lumefantrine/artemether	L-Artem forte	480/80	tablets	2
AL10	lumefantrine/artemether	Lonart DS	480/80	tablets	1
AL11	lumefantrine/artemether	Lonart forte	240/40	tablets	1
AL12	lumefantrine/artemether	Lufamet forte	240/40	tablets	1
AL13	lumefantrine/artemether	Lumart-E	120/20	dispersible tablets	1
AL14	lumefantrine/artemether	Lumartem	120/20	tablets	15
AL15	lumefantrine/artemether	Mefanther DS	480/80	tablets	1
AL16	lumefantrine/artemether	Mefanther Forte	240/40	tablets	1
F1	falsified	Coartem	120/20	tablets	3
F2	falsified	Combiart	120/20	tablets	2

The paracetamol combination sample colors correspond to colors used in Figure 3

Table 3 : Figures of merit of NIR and Raman systems for HQI model

	IBUPROFEN				PARACETAMOL				COARTEM			
Metrics	**NIR-A**	**NIR-B**	**Raman-A**	**Raman-B**	**NIR-A**	**NIR-B**	**Raman-A**	**Raman-B**	**NIR-A**	**NIR-B**	**Raman-A**	**Raman-B**
spectral range (cm^{-1})	6500-5000	9143-6399	284-1825	420-1800	9797-4397	9143-6399	284-1825	420-1800	9797-4397	9143-6399	284-1825	420-1800
preprocessing	SG(1,2,15) UA	SG(1,2,5) UA	SG(1,2,35) SNV	SG(1,2,25) SNV	SG(1,2,15) UA	SG(1,2,5) UA	SG(1,2,35) SNV	SG(1,2,25) SNV	SG(1,2,15) UA	SG(1,2,5) UA	SG(1,2,15) SNV	SG(1,2,25) SNV
TP	80	80	80	80	86	94	100	100	70	70	70	70
TN	333	322	240	244	581	444	82	180	255	287	26	172
FP	7	18	100	96	9	146	508	410	165	133	394	248
FN	0	0	0	0	14	6	0	0	0	0	0	0
Matthews correlation coefficient	0.949	0.879	0.560	0.571	0.944	0.512	0.151	0.245	0.425	0.485	0.097	0.300

SG: Savitzky-Golay (derivative, polynomial order, window size)

UA: unit area normalization

SNV: standard normal variate

Table 4 : Figures of merit of NIR and Raman systems for DD-SIMCA model

	IBUPROFEN				PARACETAMOL				COARTEM			
Metrics	**NIR-A**	**NIR-B**	**Raman-A**	**Raman-B**	**NIR-A**	**NIR-B**	**Raman-A**	**Raman-B**	**NIR-A**	**NIR-B**	**Raman-A**	**Raman-B**
spectral range (cm^{-1})	6500-5000	9143-6399	284-1825	420-1800	9797-4397	9143-6399	284-1825	420-1800	9797-4397	9143-6399	284-1825	420-1800
preprocessing	SG(1,2,15) UA	SG(1,2,5) UA	SG(1,2,35) SNV	SG(1,2,25) SNV	SG(1,2,15) UA	SG(1,2,5) UA	SG(1,2,35) SNV	SG(1,2,25) SNV	SG(1,2,15) UA	SG(1,2,5) UA	SG(1,2,15) SNV	SG(1,2,25) SNV
# PC	1	1	2	3	1	1	6	5	1	1	2	3
α	1x10-5	1x10-3	1x10-6	1x10-4	1x10-4	2x10-2	1x10-4	1x10-4	1x10-5	1x10-4	1x10-3	1x10-4
TP	80	80	77	60	100	95	96	95	70	60	69	69
TN	340	340	340	340	590	590	574	311	420	430	258	285
FP	0	0	0	0	0	0	16	279	0	0	162	135
FN	0	0	3	20	0	5	4	5	0	0	1	1
Matthews correlation coefficient	1,000	1,000	0.977	0.842	1,000	0.971	0.891	0.337	1,000	1,000	0.421	0.472

SG: Savitzky-Golay (derivative, polynomial order, window size)

UA: unit area normalization

SNV: standard normal variate

Fig. S.1. G-I DD-SIMCA acceptance plots:

(A) NIR-A: autoscaling, 1 PC, α=0.00001

(B) NIR-B: autoscaling, 1 PC, α=0.001

(C) Raman-A: autoscaling, 2 PC, α=0.000001

(D) Raman-B: autoscaling, 3 PC, α=0.0001

"G" samples are the reference artemether-lumefantrine samples; "I" samples are the ibuprofen samples; "P" samples are the paracetamol and paracetamol combination samples; "AL" samples are the artemether-lumefantrine samples and "F" samples are the falsified samples (for more details the reader is referred to Table 2).

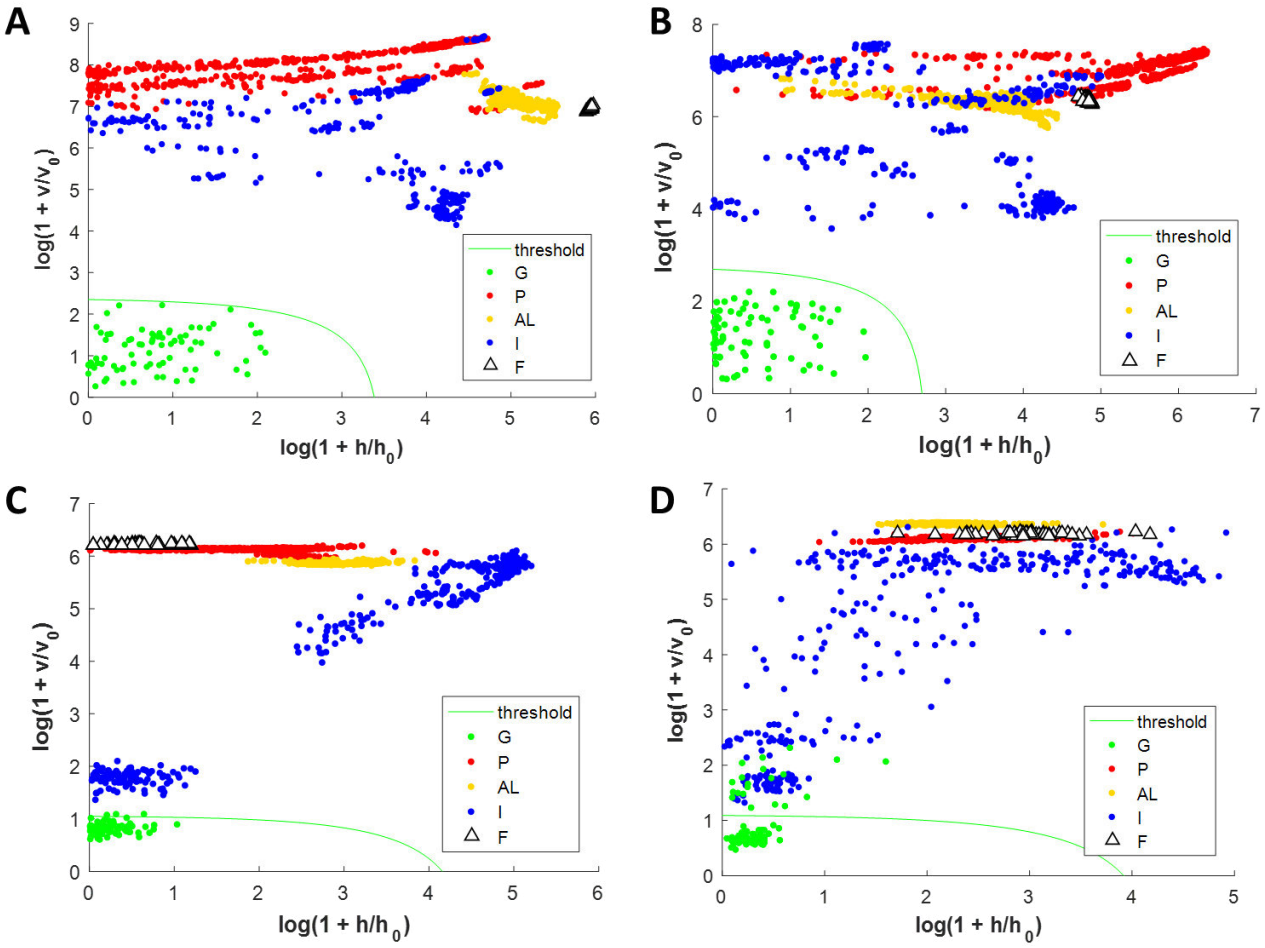

Fig. S.2. G-P DD-SIMCA acceptance plots:

(A) NIR-A: autoscaling, 1PC, α=0.0001

(B) NIR-B: autoscaling, 1PC, α=0.02

(C) Raman-A: autoscaling, 6PC, α=0.0001

(D) Raman-B: autoscaling, 5PC, α=0.0001

"G" samples are the reference artemether-lumefantrine samples; "I" samples are the ibuprofen samples; "P" samples are the paracetamol and paracetamol combination samples; "AL" samples are the artemether-lumefantrine samples and "F" samples are the falsified samples (for more details the reader is referred to Table 2).

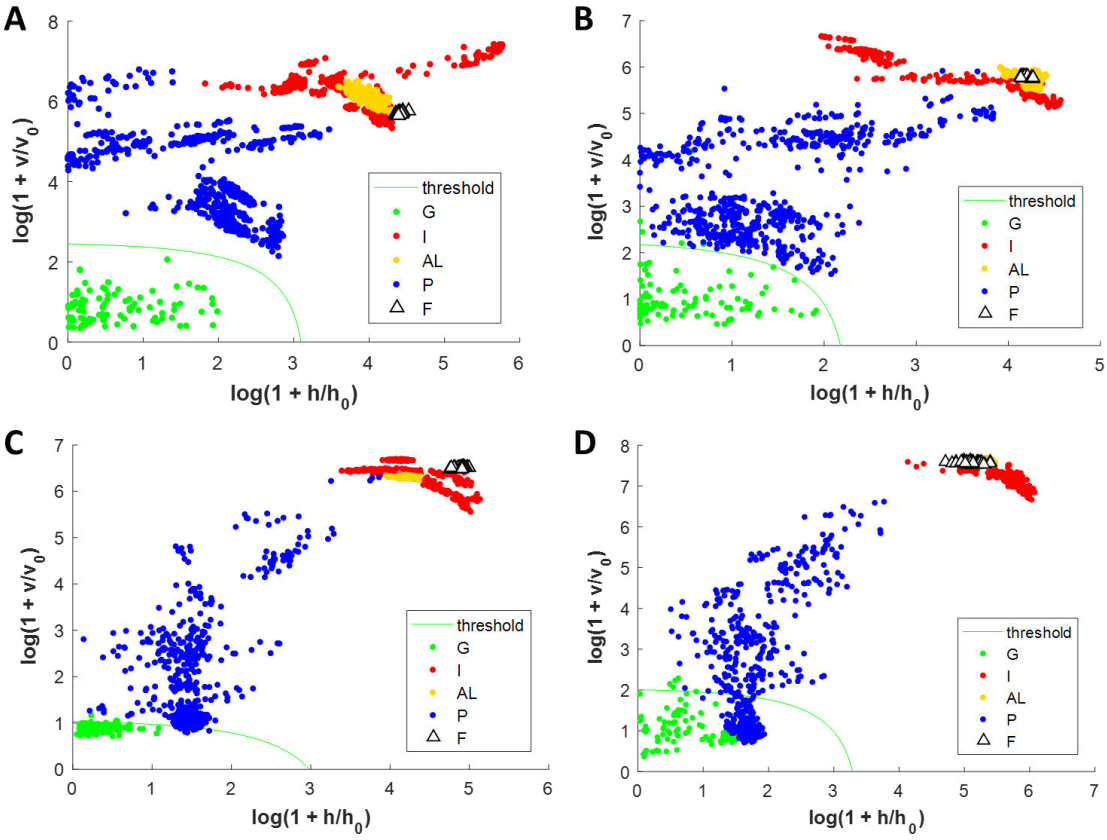

Table S1. HQI mean results for NIR and Raman systems

Code	NIR-A (mean HQI % +/- SD)			NIR-B (mean HQI % +/- SD)			Raman-A (mean HQI % +/- SD)			Raman-B (mean HQI % +/- SD)		
	Coartem 20/120 mg	Dafalgan 1g	Ibuprofen EG 400mg	Coartem 20/120 mg)	Dafalgan 1g	Ibuprofen EG 400mg	Coartem 20/120 mg	Dafalgan 1g	Ibuprofen EG 400mg	Coartem 20/120 mg	Dafalgan 1g	Ibuprofen EG 400mg
G-AL	99,8 +/- 0,1	45,9 +/- 0,9	39,3 +/- 0,7	99,9 +/- 0,1	24,0 +/- 0,2	55,8 +/- 0,6	99,4 +/- 0,0	9,0 +/- 0,1	1,8 +/- 0,1	99,2 +/- 0,3	0,1 +/- 0,0	0,0 +/- 0,0
G-P	59,4 +/- 1,1	98,0 +/- 1,1	32,4 +/- 5,3	22,1 +/- 4,2	98,4 +/- 0,7	22,0 +/- 3,5	1,8 +/- 0,1	98,8 +/- 0,0	0,1 +/- 0,0	0,9 +/- 0,1	99,4 +/- 0,4	0,0 +/- 0,0
G-I	42,9 +/- 4,1	58,3 +/- 0,7	99,2 +/- 0,4	55,6 +/- 0,9	23,9 +/- 0,4	99,8 +/- 0,1	9,0 +/- 0,1	0,1 +/- 0,0	98,4 +/- 0,1	0,0 +/- 0,0	0,0 +/- 0,0	99,5 +/- 0,1
P1		66,9 +/- NA			93,7 +/- NA			97,9 +/- NA			97,6 +/- NA	
P2		66,2 +/- 0,5			90,4 +/- 0,5			97,7 +/- 0,1			97,7 +/- 0,0	
P3		97,6 +/- 1,3			98,4 +/- 0,5			98,8 +/- 0,1			99,5 +/- 0,2	
P4		77,1 +/- 0,5			93,8 +/- 0,0			97,8 +/- 0,1			97,2 +/- 0,0	
P5		76,9 +/- 0,9			83,3 +/- 1,6			97,8 +/- 0,1			96,3 +/- 0,5	
P6		69,6 +/- 1,6			90,8 +/- 0,2			97,9 +/- 0,1			97,5 +/- 0,1	
P7		67,9 +/- 1,0			90,6 +/- 0,7			97,8 +/- 0,1			97,3 +/- 0,1	
P8		64,9 +/- NA			68,1 +/- NA			97,5 +/- NA			96,1 +/- NA	
P9		53,0 +/- NA			65,0 +/- NA			76,9 +/- NA			38,5 +/- NA	
P10		73,1 +/- 0,7			94,9 +/- 0,3			95,3 +/- 2,8			88,1 +/- 9,2	
P11		69,5 +/- 1,0			96,4 +/- 0,3			97,7 +/- 0,3			97,2 +/- 0,7	
P12	32,6 +/- 16,3	74,6 +/- 0,3	22,3 +/- 14,0	26,9 +/- 16,9	95,8 +/- 0,5	24,2 +/- 12,9	8,8 ë 0,0	97,8 +/- 0,1	0,3 +/- 0,0	0,8 +/- 0,2	97,4 +/- 0,2	0,1 +/- 0,3
P13		61,2 +/- 5,7			77,8 +/- 2,9			71,0 +/- 1,9			73,9 +/- 4,7	
P14		68,3 +/- 2,3			76,3 +/- 0,2			96,2 +/- 0,3			94,4 +/- 0,5	
P15		40,0 +/- NA			46,2 +/- NA			58,3 +/- NA			96,1 +/- NA	
P16		96,8 +/- NA			84,8 +/- NA			97,6 +/- NA			89,6 +/- NA	
P17		55,8 +/- NA			47,9 +/- NA			97,6 +/- NA			88,9 +/- NA	
P18		69,1 +/- NA			74,8 +/- NA			97,5 +/- NA			94,7 +/- NA	
P19		70,9 +/- NA			78,4 +/- NA			97,0 +/- NA			93,9 +/- NA	
P20		56,0 +/- NA			47,1 +/- NA			97,0 +/- NA			79,4 +/- NA	
P21		77,0 +/- 2,1			69,5 +/- 3,7			95,5 +/- 0,7			87,6 +/- 1,4	
P22		79,2 +/- 0,7			81,0 +/- 3,0			97,3 +/- 0,6			97,0 +/- 0,9	
P23		78,6 +/- NA			66,9 +/- NA			94,0 +/- NA			95,9 +/- NA	
I1			44,9 +/- 2,4			55,9 +/- 2,5			0,8 +/- 1,2			6,4 +/- 0,1
I2			93,8 +/- 0,5			97,0 +/- 0,6			74,8 +/- 5,9			75,8 +/- 2,8
I3			48,4 +/- 1,7			82,9 +/- 0,9			60,7 +/- 0,8			48,5 +/- 14,9
I4			85,8 +/- NA			84,1 +/- NA			97,9 +/- NA			98,7 +/- NA
I5			98,1 +/- 0,4			99,5 +/- 0,2			98,4 +/- 0,0			98,4 +/- 0,0
I6			82,7 +/- 1,9			80,5 +/- 0,6			97,6 +/- 0,1			97,0 +/- 1,2
I7	51,0 +/- 16,5	42,2 +/- 18,3	84,5 +/- NA	55,7 +/- 13,6	25,3 +/- 6,4	88,0 +/- NA	1,9 +/- 1,8	1,3 +/- 1,2	97,6 +/- NA	0,1 +/- 0,2	2,7 +/- 3,5	98,1 +/- NA
I8			66,6 +/- NA			88,4 +/- NA			85,5 +/- NA			85,0 +/- NA
I9			17,3 +/- NA			21,6 +/- NA			15,6 +/- NA			10,2 +/- NA
I10			14,8 +/- NA			23,4+/- NA			9,5 +/- NA			9,6 +/- NA
I11			80,7 +/- NA			81,7 +/- NA			75,9 +/- NA			58,3 +/- NA
I12			26,0 +/- 0,7			34,4 +/- 1,2			17,5 +/- 1,0			17,9 +/- 2,2
I13			18,0 +/- 0,8			28,8 +/- 1,5			6,7 +/- 2,6			13,9 +/- 3,7
I14			52,7 +/- 2,2			54,1 +/- 8,9			25,6 +/- 8,1			9,7 +/- 5,9
AL1	95,8 +/- 2,8			94,6 +/- 1,3			98,1 +/- 1,3			91,9 +/- 8,2		
AL2	94,7 +/- NA			94,9 +/- NA			98,9 +/- NA			94,6 +/- NA		
AL3	94,1 +/- NA			82,3+/- NA			99,3 +/- NA			96,7 +/- NA		
AL4	99,6 +/- NA			99,9 +/- NA			99,3 +/- NA			99,2 +/- NA		
AL5	95,4 +/- 1,2			97,3 +/- 0,4			99,3 +/- 0,0			99,4 +/- 0,4		
AL6	96,0 +/- NA			93,3 +/- NA			98,4 +/- NA			94,8 +/- NA		
AL7	96,3 +/- 0,0			97,3 +/- 1,0			96,7 +/- 1,4			82,8 +/- 4,2		
AL8	95,9 +/- 0,4	45,1 +/- 6,3	38,5 +/- 4,8	95,5 +/- 1,4	21,2 +/- 2,6	58,4 +/- 4,7	98,1 +/- 0,2	8,8 +/- 0,4	1,7 +/- 0,1	82,1 +/- 18,6	0,3 +/- 0,2	0,0 +/- 0,0
AL9	91,3 +/- 0,2			83,8 +/- 3,6			98,4 +/- 0,4			86,5 +/- 6,2		
AL10	93,1+/- NA			89,1 +/- NA			99,0 +/- NA			98,9 +/- NA		
AL11	94,0 +/- NA			92,9 +/- NA			92,7 +/- NA			51,5 +/- NA		
AL12	95,4 +/- NA			94,9 +/- NA			94,1 +/- NA			57,0 +/- NA		
AL13	94,7+/- NA			96,5 +/- NA			94,2 +/- NA			61,8 +/- NA		
AL14	93,7 +/- 0,6			92,0 +/- 0,8			99,3 +/- 0,1			98,4 +/- 1,4		
AL15	94,6 +/- NA			95,5+/- NA			98,8 +/- NA			94,2 +/- NA		
AL16	94,4 +/- NA			90,3 +/- NA			98,3 +/- NA			89,8 +/- NA		
C1	59,5 +/- 2,6	27,7 +/- 1,0	36,1 +/- 5,6	61,5 +/- 0,8	13,8 +/- 0,3	36,7 +/- 1,1	0,1 +/- 0,0	0,1 +/- 0,0	0,1 +/- 0,0	0,1 +/- 0,0	1,7 +/- 0,2	0,0 +/- 0,0
C2												